Published in: Nanotechnology, 2003. 14**(5): p. 551-556. And can be downloaded from (subscription required):**
http://www.iop.org/EJ/abstract/0957-4484/14/5/313

Intracellular Integration of Synthetic Nanostructures with Viable Cells for Controlled Biochemical Manipulation

Timothy E. McKnight[1], Anatoli V. Melechko[2], Guy D. Griffin[3], Michael A. Guillorn[1], Vladimir I. Merkulov[1], Francisco Serna[1], Dale K. Hensley[1], Mitchel J Doktycz[3], Douglas H. Lowndes[4], and Michael L. Simpson[1,5]

[1]Molecular-Scale Engineering and Nanoscale Technology Research Group, Oak Ridge National Laboratory, Oak Ridge, Tennessee 37831

[2]Department of Electrical and Computer Engineering, University of Tennessee, Knoxville, Tennessee 37996

[3]Life Sciences Division, Oak Ridge National Laboratory, Oak Ridge, Tennessee 37831

[4]Condensed Matter Sciences Division, Oak Ridge National Laboratory, Oak Ridge, Tennessee 37831

[5]Also affiliated with Materials Science and Engineering Department, University of Tennessee, Knoxville, Tennessee 37996

Abstract

We demonstrate the integration of vertically aligned carbon nanofiber (VACNF) elements with the intracellular domains of viable cells and controlled biochemical manipulation of cells using the nanofiber interface. Deterministically synthesized VACNFs were modified with either adsorbed or covalently-linked plasmid DNA and were subsequently inserted into cells. Post insertion viability of the cells was demonstrated by continued proliferation of the interfaced cells and long-term (> 22 day) expression of the introduced plasmid. Adsorbed plasmids were typically desorbed in the intracellular domain and segregated to progeny cells. Covalently bound plasmids remained tethered to nanofibers and were expressed in interfaced cells but were not partitioned into progeny, and gene expression ceased when the nanofiber was no longer retained. This provides a method for achieving a genetic modification that is non-inheritable and whose extent in time can be directly and precisely controlled. These results demonstrate the potential of VACNF arrays as an intracellular interface for monitoring and controlling subcellular and molecular phenomena within viable cells for applications including biosensors, *in-vivo* diagnostics, and *in-vivo* logic devices.

1. Introduction

An emerging goal of postgenomic research is the development of an understanding of gene circuit and network structure and function that give rise to complex cell functionality. To date, work in this direction has been focused on the analysis, modelling, and simulation of gene circuits [1] or the development of synthetic gene circuits which mimic electronic functionality [2] such as a toggle switch [3], an

oscillator [4], or combinatorial logic gates [5,6]. While these software and 'cellware' elements provide invaluable tools for the exploration of gene circuit and network structure and function, the missing elements are hardware tools that close the feedback loop between simulation and experiment. Such tools are considered indispensable in the analogous field of electronic device modelling, and are likely to play a similar role in genetic circuit modelling and design. The ideal tools would interface directly with the appropriate biomolecular processes, allow the introduction of stimuli, and provide transduction of responses with both spatial and temporal resolution, all performed without adversely affecting cell viability or functionality.

Engineered nanoscale devices may provide realization of these tools for monitoring and manipulating cellular processes, as they reside at the same size scale as the biomolecular machines of cells. Such an interface of nanotechnology and biotechnology has been demonstrated by using non-bleaching fluorescent nanocrystals in place of dyes for monitoring cellular processes [7-9]. Pulled glass capillaries with nanoscale tips have also been implemented for cellular and subcellular electrophysiological monitoring [10] and for biochemical manipulation of cells via microinjection of membrane-impermeable molecules (e.g. proteins, DNA) [11]. While these nanoscale interfaces have dramatically increased our knowledge of cellular processes, they typically are limited to techniques that require manipulating cells one at a time using individual elements observed under a microscope, and thus typically provide only a serial interface to cells. Parallel embodiments of these devices have been fabricated using silicon microfabrication methods [12], but, as with all micromachining techniques, there are limitations to the ultimate size scale and density of features (tip radii and spacing of the silicon needles) and a limited choice of substrate materials which are often not well-suited to cell culture or observation due to material incompatability or optical opacity.

Carbon nanotubes (CNTs) and related nanostructures provide a new approach to nano- and microdevice fabrication that avoid many of the limitations of micromachining while providing the means to construct addressable functional nanoscale devices including chemically specific AFM probes [13,14], electrochemical probes [15], and electromechanical manipulators [16]. Within this family of structures, carbon nanofibers are uniquely suited for the construction of intracellular devices because of the ability to exquisitely control their synthesis. Deterministic arrays of closely-spaced (pitch ≥ 1 μm) vertically aligned carbon nanofibers (VACNFs) [17-19] may be grown on a wide variety of substrates (including quartz and glass slides) with wide bases that provide mechanical strength while still generating a small diameter tip (≥ 5 nm tip radius) appropriate for insertion directly into cells. In this article, we show a critical enabling step toward the hardware tools needed for the coupling of gene circuit simulation with experiment by demonstrating the functional integration of VACNF elements within cells. The viability of the cells after VACNF insertion is demonstrated by the long-term expression of a constitutively-expressed green fluorescent protein (GFP) gene carried on nanofiber-borne plasmid molecules. This hybrid combination of cell and nanostructure accomplished gene expression from plasmid DNA both adsorbed and tethered to the VACNFs, where tethered plasmid molecules were not partitioned into progeny after cell division. This provides a method for achieving a genetic modification that is non-inheritable and whose extent in time can be directly and precisely controlled. In addition to gene circuit characterization, this capability may address other more general genetic manipulation needs such as controlling the time course of gene expression during critical cell or embryo development [20].

2. Materials and Methods

Vertically-aligned nanofiber arrays were synthesized from 500 nm diameter nickel catalyst dots that were photolithographically defined at 5 μm intervals on 100 mm, n-type silicon wafers. VACNF growth was accomplished using a previously described plasma-enhanced chemical vapor deposition process [18,19]. In brief, the wafer was maintained at a temperature of 700 deg C, while a mixture of C_2H_2 and NH_3 was introduced into a PECVD chamber at 3 Torr of total pressure. The plasma was initiated and maintained at 450 V and 300 mA. Growth of individual fibers resulted from catalytic deposition of carbonaceous material through the nickel particle at the growing-fiber tip, and deposition of carbonaceous material on the fiber surface. The ammonia served as an etchant to remove a passivating carbon film that continuously forms on the surface of the catalyst particle, and also as a source of nitrogen doping for the growing structure. Typical growth resulted in conically-shaped fibers of 6-10 μm length (depending upon growth time) with tip diameters of 20-50 nm and base diameters of 500-600 nm. Following nanofiber growth, the wafers were cleaved into 3 mm x 3 mm chips that were covered with VACNFs arrays with a 5-μm pitch (Fig. 1a).

Following synthesis, nanofiber arrays were surface-modified with plasmid DNA. The plasmid used in these experiments was pGreenLantern-1 (previously available as Cat # 10642-015, Gibco BRL, Gaithersburg, MD) which contains an enhanced green fluorescent protein (eGFP) gene with the CMV immediate early enhancer/promoter and SV40 t-intron and polyadenylation signal. Plasmid DNA at various concentrations (5-500 ng/μl) was either spotted onto the chips as 0.5-1 μl aliquots and allowed to dry or covalently tethered to the nanofibers. For covalent attachment, VACNF arrays were etched for 5 min in an RF oxygen plasma to provide oxygen-containing moieties, including carboxylic acid groups, on the nanofiber surface. The chips were covered with 1 ml of 0.1M MES buffer (2-[N-morpholino]ethane sulfonic acid at a pH of 4.5)

containing 10 mg of EDC (1-ethyl-3-(3-dimethylaminopropyl)carbodiimide) and 1 μg of plasmid DNA. This reaction mixture was agitated on an orbital shaker for two hours at room temperature to condense primary amines on DNA to the carboxylic acid sites of oxygen plasma etched fibers [21,22]. In parallel, control samples were prepared identically except no EDC was used during the incubation step. Both sample types were then rinsed extensively in phosphate buffered saline and water to remove non-specifically adsorbed DNA.

The cell line used predominantly for these experiments was a subclone of the Chinese hamster ovary (CHO), designated K_1-BH_4 and provided to us by Dr. A.W. Hsie [23]. Cells were routinely grown in Ham's F-12 nutrient mixture (Cat.# 11765-054, GibcoBRL, Gaithersburg, MD) supplemented with 5% fetal bovine serum (qualified, heat-inactivated, Cat.# 16140-071, GibcoBRL) and 1 mM glutamine (Cat.# G-6392, Sigma Chemical Co., St Louis, MO). Cell cultures were grown in T-75 Flasks (Falcon #3111, Becton Dickinson & Co, Franklin Lakes, NJ) and passaged at 80% confluency by trypsinization using trypsin-EDTA (Cat# 15305-014, GibcoBRL). In preparation for fiber-mediated plasmid delivery, adherent cells were trypsinized from T-75 flasks, pelleted at 100G for 10 min, resuspended in phosphate buffered saline (PBS), counted, and diluted in PBS to a desired density ranging from 50,000 to 600,000 cells/ml.

To interface cells to DNA modified nanofiber arrays, CHO cells were centrifuged at 600 G out of suspension in PBS onto these chips, which resulted in some cellular impalement on VACNFs (Fig 1b). Optionally, to increase the probability and depth of fiber penetration into cells, the chip was gently pressed against a flat, wetted surface following the spin (Fig 1c). Following these integration steps, the chip was placed in growth media in a culture dish and incubated to allow cell recovery and proliferation (Fig 1d).

3. Results and Discussion

In these experiments, we employed the expression of a reporter gene, GFP, to indicate successful intracellular integration and delivery of plasmid DNA by the fiber and to provide a marker for continued viability of the interfaced cell. For this approach to work, the nanofiber array must retain DNA during cellular manipulations, penetrate the membrane boundary of cells, and deliver DNA to the intracellular domain. Finally, the delivered plasmid DNA must also be expressed within the recipient/interfaced cells.

CHO cells are approximately 7 μm diameter spheres while in suspension. As such, nanofiber arrays were synthesized at a pitch of 5 μm, such that, during centrifugation and the optional press step, a cell would likely interact directly with only a few nanofibers. Typical results of these interactions are shown in Fig 2. Immediately following centrifugation, cells retained their rounded shape and were loosely coupled with the chip (Fig 2a). When the press step was used, the cells tended to deform from their spherical shape and attach to the nanofibers and interfiber surfaces of the substrate (Fig 2b). In either case, the cells eventually began to attach and stretch out on the substrate and continue to proliferate (Fig 2c).

Following a culture period of at least 24 hours, the interaction of plasmid-spotted nanofibers and cells was evaluated by observing plasmid-coded GFP expression with fluorescence microscopy. When cells were centrifuged onto the array at 600G, GFP expression (GFP+) was detected in cells at only a very low frequency (<1% of the cells on the fibered substrate). Pelleting forces were increased to as high as 5000G with no apparent increase in GFP+. Increasing the pelleting forces further resulted in significant

cell death and the inability of surviving cells to recover from the pelleting process. Using a moderate pelleting force (600G) to position cells upon the nanofiber array, and then including a subsequent press step (Fig 2b) typically increased the number of GFP+ cells, often by as much as a factor of 5 and occasionally even more significantly, with some tests resulting in ~50% of the cells on the substrate being GFP+. While the press step introduced much variability in the yield of GFP+ cells, it appeared necessary in order to cause fiber penetration (and DNA delivery) into the intracellular domain.

An important factor influencing the amount of GFP+ observed following these integration steps was nanofiber composition. In general, nanofibers comprised exclusively of carbon resulted in extremely low yields of GFP+ cells (<<1%) – even using the press step to increase fiber penetration. This low yield appears to not be indicative of low probability of fiber penetration into cells, but rather due to low retention of DNA on these structures and loss of plasmid prior to cell/fiber interaction. In fluorescent tagging and gel-electrophoresis-based studies of plasmid adsorption and desorption from VACNFs, carbon-based VACNFs did not retain DNA during even gentle washing (data not shown). The surface chemistry of nanofibers, however, may be altered during synthesis to feature high levels of nitrogen content, ranging from essentially 0 to more than 50 atomic % as measured by energy dispersive x-ray spectroscopy [24]. In contrast to the poor DNA retention of exclusively *carbon* nanofibers, nitrogen-containing VACNFs retained DNA during repeated washing, presumably due to electrostatic interactions between the anionic phosphate backbone of the DNA and the nitrogen-bearing sites on the nanofibers. It is with nitrogen-bearing nanofiber arrays that the relatively high-yields of GFP+ were observed.

Using nitrogen-bearing nanofibers that had been spotted with plasmid DNA, reproducible GFP expression patterns were observed following cell recovery and proliferation. For the chips that were pressed following centrifugation, GFP+ cells and

clusters were observed both on the chip and also in regions of the culture dish off the chip. These latter GFP+ cells had apparently received plasmid from VACNFs but had disassociated from the chip and reattached elsewhere in the culture dish during manipulations. Both on and off-chip, as a GFP+ cell divided, delivered plasmid would be segregated to progeny, which in turn would express GFP. Plasmid segregation was observed with the formation of GFP+ cell clusters, and often these clusters would result in large, potentially stable colonies of GFP+ cells, as shown in Fig 3. This colony resulted from the merging of three separate clusters of GFP+ cells on a chip that only had 20 initial GFP+ cells 24 hrs after being placed on the chip. This relatively high probability for potentially stable colony formation may be due to plasmid DNA being delivered directly to the nuclear domain. In CHO cells the nuclear target (2-3 μm diameter) can be a substantial fraction of the cell's overall projected area (7 μm diameter). Thus, nuclear impalement may frequently coincide with cellular impalement by the nanofibers.

In contrast to these results, an intriguing observation was that occasionally a GFP+ cell on the chip did not generate any GFP expressing progeny, even over relatively long time periods (22 days). In these cases, it appeared plasmids were being retained and expressed by the original GFP+ cell, but were not being segregated to progeny cells. We postulated that this behavior was due to VACNF penetration and delivery of plasmid DNA directly into the nuclear domain but without release of the plasmid from the VACNF and therefore without subsequent partitioning into progeny. Rather, these plasmid molecules may have been immobilized on the nanofibers due to multiple electrostatic interactions [25] at portions of their circular structure while other, active coding regions of these same plasmids remained unbound and accessible for transcriptional activity. For the plasmid used in these experiments, the active mammalian coding regions are only about 30% of the overall plasmid length. With a large number of plasmids on each nanofiber, it is likely that some plasmid molecules

were positioned such that the GFP site was available for polymerase binding and transcription.

To test this model we prepared VACNF chips with plasmid DNA covalently linked to the VACNFs such that there would be minimal free plasmid available for segregation to progeny. We conducted our centrifugation and press integration method using using four chips with plasmids covalently bound to the VACNFs using an EDC-condensation reaction and four control chips that had been incubated with the DNA reaction mixture, but without the EDC catalyst. Both sample types were extensively rinsed following the incubation step. For the control samples, without EDC in the reaction mix, there should be no covalent binding of DNA to the nanofiber scaffold and subsquent extensive rinsing would remove non-specifically bound DNA from the nanofibers. Following centrifugation and pressing of cells onto these fibered chips, the covalently-linked samples resulted in 81, 198, 65, and 102 GFP+ cells on each chip, respectively. The control samples resulted in no GFP+ cells on three chips and one faint GFP+ cell on the fourth, indicating that non-specifically adsorbed plasmid DNA had effectively been removed from the samples during rinse steps. Unlike previous experiments with samples non-covalently spotted with plasmid, no off-chip GFP+ cells were observed, indicating that GFP expression required the *continued* retention of the DNA-derivitized VACNF element within the cell.

Fig. 4a illustrates the dramatic differences in GFP expression from cells integrated with VACNFs with either spotted (top) or covalently linked DNA (bottom). The spotted sample produced colonies of GFP+ cells from initial transfectants while the covalently linked sample maintained a nearly constant number of GFP+ cells over a 22 day period (days 7 and 14 shown). While growth and proliferation is occurring in both cases, the covalently bound plasmid is not available for segregation to progeny, and only the cells that retain a plasmid-derivatized nanofiber remain GFP+. Fig. 4b follows a typical cell

on a covalently linked chip. Between day 7 and 8, this cell divided, and the mother cell (denoted '1') continued to fluoresce for several days, indicating the continued expression of GFP. Fluorescence continued in the progeny cell (denoted '2') after division, presumably due to partitioning of the GFP protein. However, this fluorescence decreased and ultimately ceased within approximately one day, indicating the decay of the partitioned protein and the absence of new GFP synthesis. The GFP- daughter cell was still present on the chip as seen in bright field optical images (fig. 4c).

4. Conclusion

We have shown that arrays of carbon nanofiber elements may be functionally integrated within cells which remain viable after VACNF insertion. This successful integration provides an intracellular biochemical interface that is a critical enabling step in the realization of hardware tools that couple modelling and experiment in genetic circuit and network exploration and design. While the functioning of this hybrid combination of cell and synthetic nanostructure was demonstrated by observing long-term gene expression from nanofiber-bound plasmid molecules, it demonstrates that other functional properties of VACNFs may be used during intracellular deployment without compromising cell viability. For example, previously demonstrated VACNF electrochemical probes [15] could be deployed within cells, or electronically or heat activated methods [26] for binding or releasing the active coding regions of the delivered plasmid to the nanofiber could provide very specific temporal control of gene expression. Additionally, in our experiments there was evidence of a high incidence of nuclear delivery of plasmid using VACNF vectors. If so, this would overcome a lack of nuclear targeting and may shield delivered DNA from cytosolic degradative pathways, each of which are frequently cited as a limitations of transfection methods [27]. Application of both intracellular control elements and efficient DNA delivery go well beyond applications of gene circuit and network probing. For example, VACNF-

mediated delivery may prove useful when other transfection methods are toxic to the cell [28], or where the expression of a delivered gene is needed for a limited but well controlled time period for the optimized development of a cell or embryo [20]. In any of these applications, the controlled synthesis and directed assembly of synthetic nanoscale structures provide the means to directly manipulate bimolecular processes in cells or to bridge the gap between informational pathways in living and synthetic systems. Advances in this coupling of nanotechnology and biotechnology hold the promise of providing flexible methods for genetically manipulating cells and providing deeper insights into the complex systems which give rise to cellular function.

References

1. D. Endy, R. Brent, *Nature* **409**, 391 (2001).
2. J. Hasty, D. McMillen, J. J. Collins, *Nature* **420**, 224 (2002).
3. T. S. Gardner, C. R. Cantor, J. J. Collins, *Nature* **403**, 339 (2000).
4. M. B. Elowitz, S. Leibler, *Nature* **403**, 335 (2000).
5. C. C. Guet, M. B. Elowitz, W. H. Hsing, S. Leibler, *Science* **296**, 1466 (2002).
6. M. L. Simpson, G. S. Sayler, J. T. Fleming, B. Applegate, *Trends in Biotechnology* **19**, 317 (2001).
7. W. C. W. Chan, S. M. Nie, *Science* **281**, 2016 (1998).
8. M. Bruchez, M. Moronne, P. Gin, S. Weiss, A. P. Alivisatos, *Science* **281**, 2013 (1998).
9. B. Dubertret *et al.*, *Science* **298**, 1759 (2002).
10. R. M. Wightman *et al.*, *Proc. Natl. Acad. Sci. U.S.A.* **88**, 10754 (1991).
11. M. Knoblauch, J. M. Hibberd, J. C. Gray, A. J. E. van Bel, *Nature Biotechnol.* **17**, 906 (1999).
12. D. V. McAllister, M. G. Allen, M. R. Prausnitz, *Annu. Rev. Biomedical Engin.* **2**, 289 (2000).
13. S. S. Wong, E. Joselevich, A. T. Woolley, C. L. Cheung, C. M. Lieber, *Nature* **394**, 52 (1998).
14. A. T. Woolley, C. Guillemette, C. L. Cheung, D. E. Housman, C. M. Lieber, *Nature Biotechnol.* **18**, 760 (2000).
15. M. A. Guillorn *et al.*, *J. Appl. Phys.* **91**, 3824 (2002).
16. P. Kim, C. M. Lieber, *Science* **286**, 2148 (1999).
17. Z. F. Ren *et al.*, *Science* **282**, 1105 (1998).
18. V. I. Merkulov, D. H. Lowndes, Y. Y. Wei, G. Eres, E. Voelkl, *Appl. Phys. Lett.* **76**, 3555 (2000).
19. V. I. Merkulov, M. A. Guillorn, D. H. Lowndes, M. L. Simpson, E. Voelkl, *Appl. Phys. Lett.* **79**, 1178 (2001).

20. B. Cong, J. Liu, S. D. Tanksley, *Proc. Natl. Acad. Sci. U.S.A.* **99**, 13606 (2002).
21. C. Dwyer *et al.*, *Nanotechnology* **13**, 601 (2002).
22. C. V. Nguyen *et al.*, *Nano Letters* **2**, 1079 (2002).
23. A. W. Hsie *et al.*, *Mutat. Res.* **86**, 193 (1981).
24. V. I. Merkulov, A. V. Melechko, M. A. Guillorn, D. H. Lowndes, M. L. Simpson, *Appl. Phys. Lett.* **80**, 476 (2002).
25. G. M. Brown *et al.*, *Ultramicroscopy* **38**, 253 (1991).
26. K. Hamad-Schifferli, J. J. Schwartz, A. T. Santos, S. G. Zhang, J. M. Jacobson, *Nature* **415**, 152 (2002).
27. D. Luo, W. M. Saltzman, *Nature Biotechnol.* **18**, 33 (2000).
28. M. C. Filion, N. C. Phillips, *Int. J. Pharm.* **162**, 159 (1998).

Acknowledgements

The authors wish to thank P. Fleming for nanofiber substrate preparation, S.Patterson for generation and purification of plasmid DNA, and T. Kuritz for initial investigations with prokaryotic systems. This work was supported in part by the National Institute for Biomedical Imaging and Bioengineering under assignment 1-R01EB000433-01 and through the Laboratory Directed Research and Development funding program of the Oak Ridge National Laboratory, which is managed for the U.S. Department of Energy by UT-Battelle, LLC.

Figure Captions

Figure 1. Structures and process used for the integration and biochemical modification of cells. **A** Carbon nanofiber array lithographically defined and synthesized in a plasma enhanced chemical vapor deposition (PECVD) process featuring 5 μm spaced, 7 μm tall fibers with tip diameters of 30 nm. **B**, Cells are spun out of a suspension in PBS onto a VACNF substrate. **C**, Following the spin, the substrate may be pressed against a wetted, flat surface. **D**, The cell covered substrate is placed face up in a culture dish, covered with growth media, and incubated for at least 24 hours prior to fluorescent imaging.

Figure 2. Scanning electron micrographs of cells following **A**, centrifugation, **B**, press, and **C**, culture for 48 hours.

Figure 3. Fluorescent micrograph of a large, potentially stable GFP+ colony 22 days after cellular integration with a plasmid spotted nanofiber array.

Figure 4. Fluorescent micrographs of CHO cells expressing VACNF-delivered GFP plasmid. **A**, Time-lapse images of GFP+ cells from (top) spotted (non-specifically adsorbed plasmid) nanofibers, and (bottom) nanofibers with covalently linked plasmid. The spotted samples tend to produce colonies of cells from initial transfectants while the covalently linked samples tend to maintain a constant number of GFP+ cells. **B**, A time-lapse sequence of a typical cell division on a covalently linked plasmid VACNF array indicating that plasmid DNA is not segregated to progeny cells. Within one day after cell division, no fluorescence is observed from the daughter cell not retained on the nanofiber. **C**, Brightfield image demonstrates that the daughter cell still resides adjacent to the mother cell. This division and subsequent loss of GFP expression in the daughter cells for covalently-linked plasmid VACNF samples maintains constant numbers of GFP+ cells over long periods of time, as indicated in the lower two panels of part **a**.

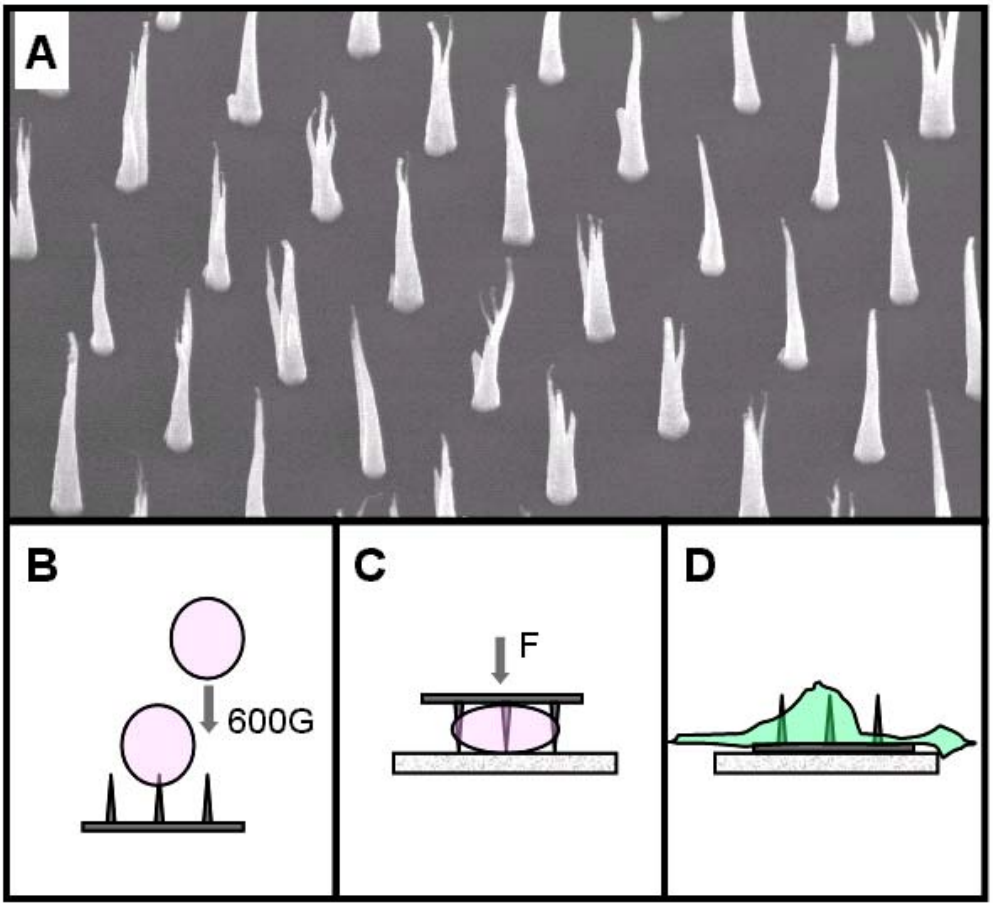

Figure 1.

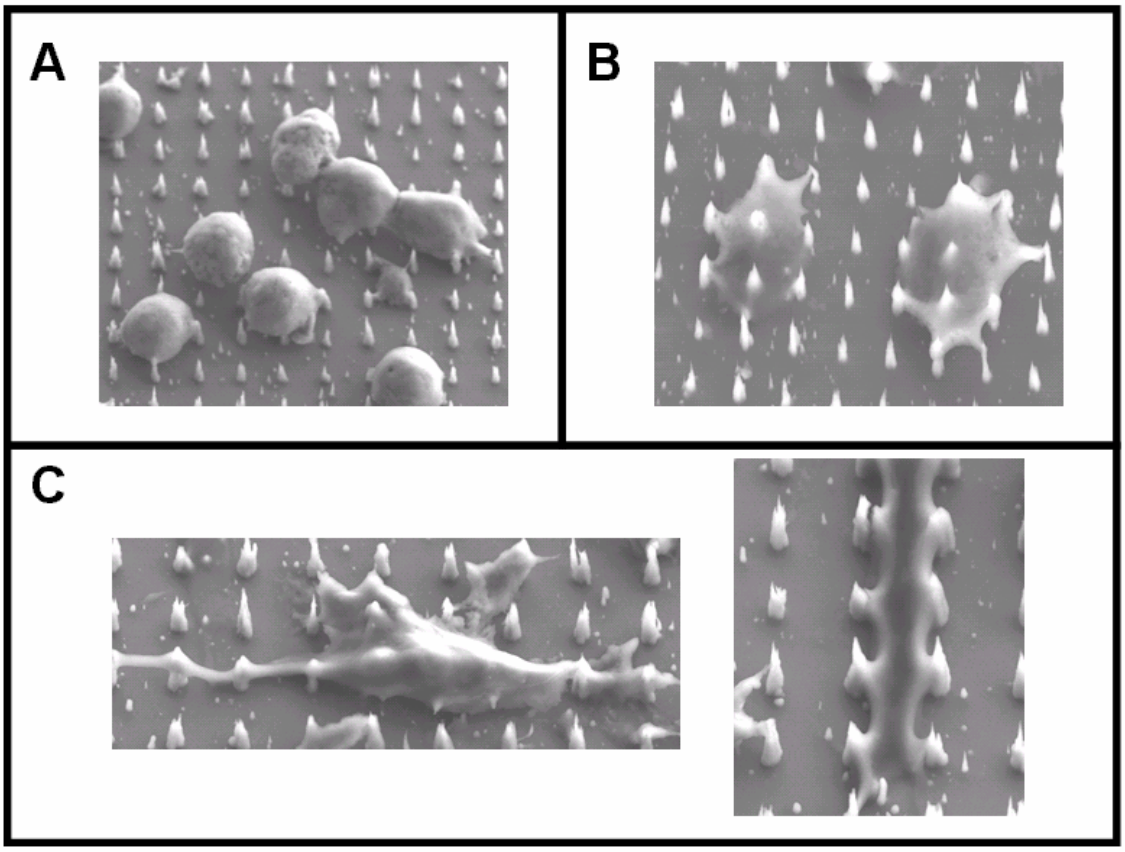

Figure 2.

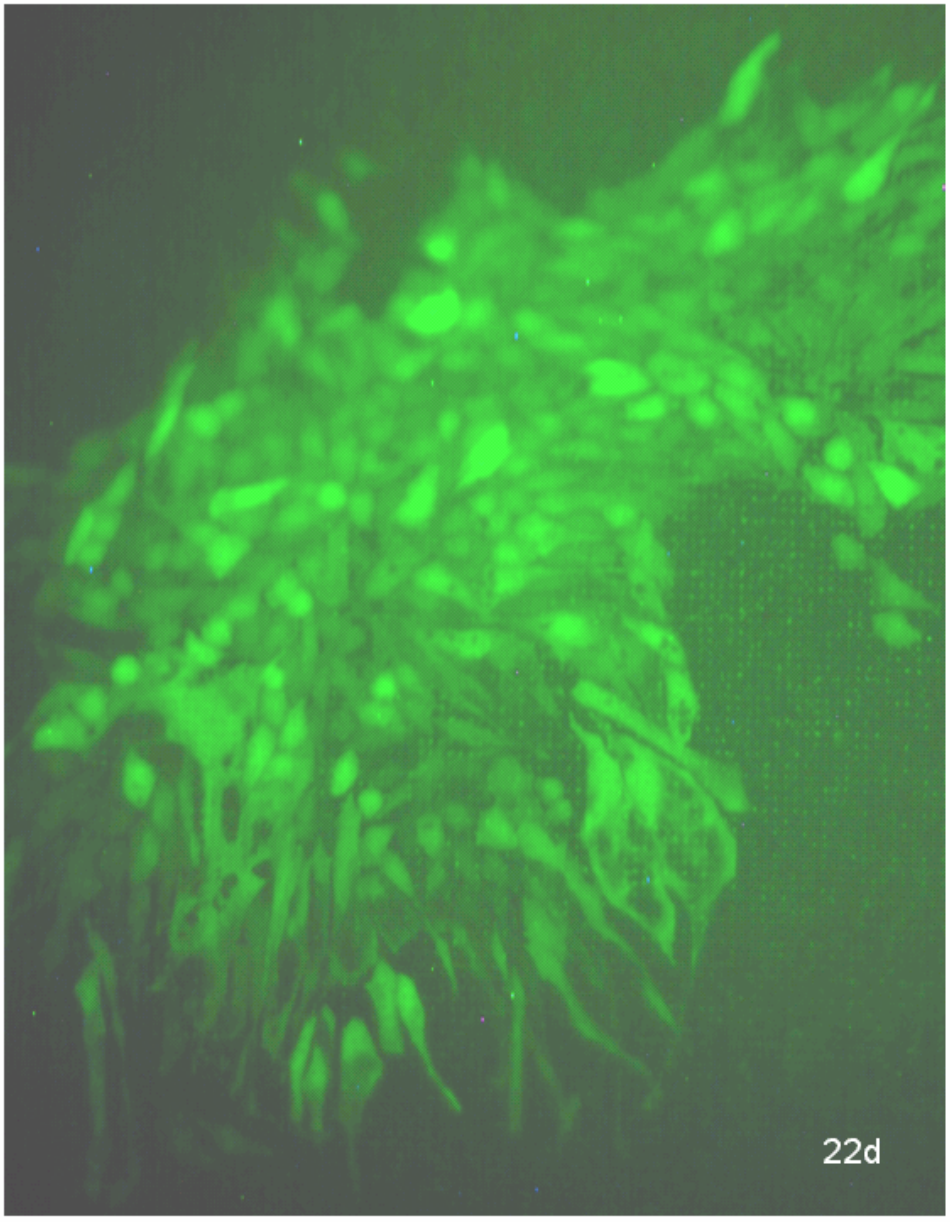

Figure 3.

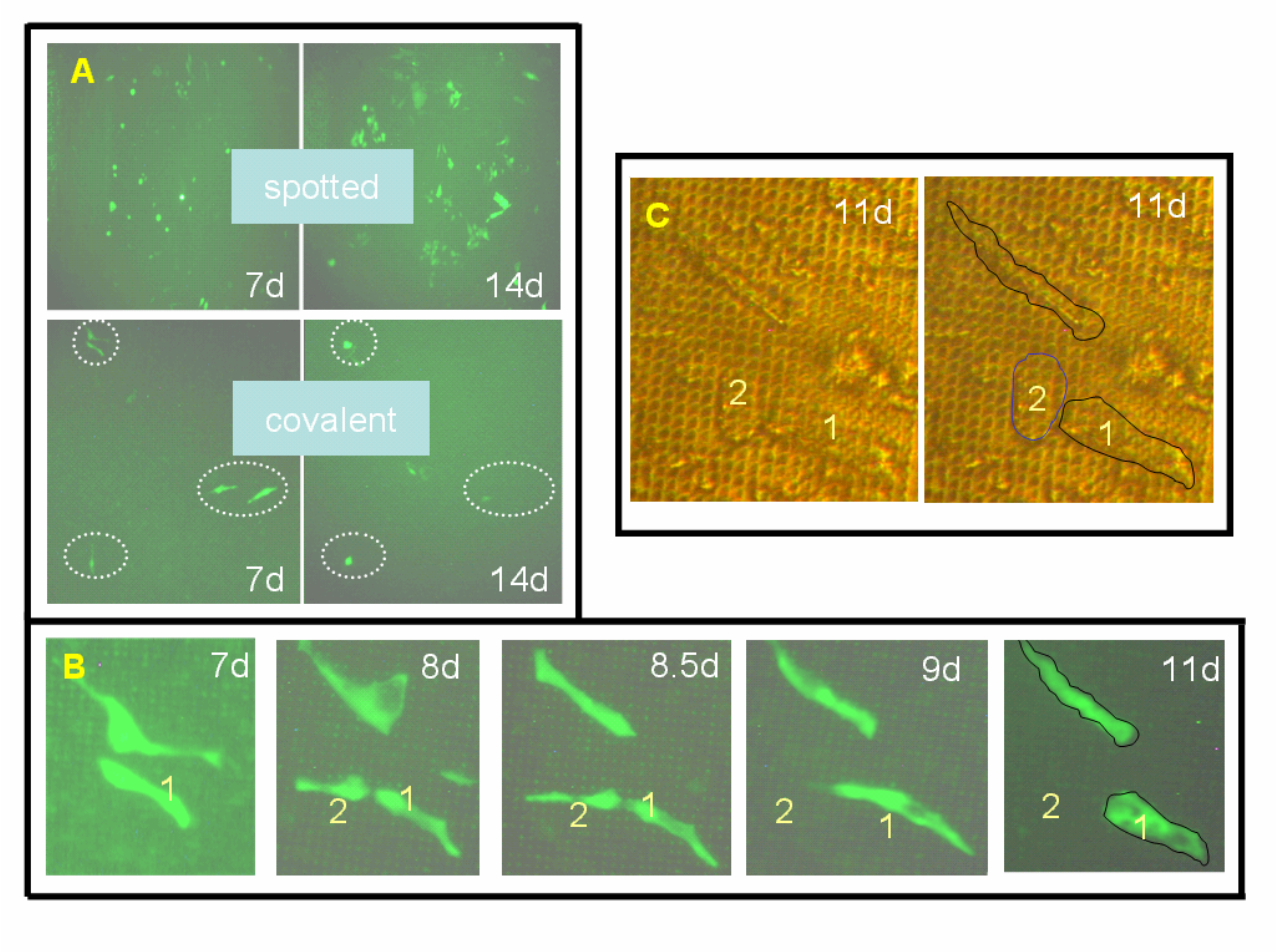
A
spotted
7d
14d
covalent
7d
14d
C
11d
2
1
11d
2
1
B
7d
1
8d
2
1
8.5d
2
1
9d
2
1
11d
2
1

Figure 4.